LA-UR-86-3827

Nov. 1986

TITLE ONE-DIMENSIONAL EASY-PLANE MAGNETS: CLASSICAL SINE-GORDON THEORY OR A QUANTUM MODEL?

AUTHOR(S) G. M. Wysin
A. R. Bishop

SUBMITTED TO Proceedings of the CNLS Sixth Annual Conference "Nonlinearities in Condensed Matter," held in Los Alamos, May 4-9, 1986.

Los Alamos Los Alamos National Laboratory
Los Alamos, New Mexico 87545

FORM NO 836 R4
ST NO 2629 5/81

One-Dimensional Easy-Plane Magnets: Classical sine-Gordon Theory or a Quantum Model?

G. M. Wysin and A. R. Bishop
Los Alamos National Laboratory
Los Alamos, NM 87545

Abstract

A classical mechanics description of one-dimensional easy-plane ferro- and antiferromagnets predicts the existence of sine-Gordon kink excitations in these systems, for the case of a small applied field within the ("strong") easy plane. Here we consider:

i) the deviations from the sine-Gordon model, due to stronger fields or weaker anisotropy, which result in modified kink properties, including negative effective masses and kink-antikink annihilation and reflection during collisions, and,

ii) equilibrium thermodynamics, especially specific heat, for quantum spin S = 1/2, and S = 1 models, comparing with the predictions of classical sine-Gordon theory and with available experimental results.

The applicability of a sine-Gordon model versus a quantum model or the full classical magnetic Hamiltonian is discussed, for materials such as $CsNiF_3$, CHAB $[(C_6H_{11}NH_3)CuBr_3]$ and TMMC $[(CD_3)_4NMnCl_3]$.

I. Introduction

There is continued strong experimental and theoretical interest in nonlinear excitations supported by low-dimensional magnetic materials. This is because of their beguilingly direct connections to model theories, such as the sine-Gordon (SG) equation in 1-dimension [1] or the Kosterlitz-Thouless scenario of vortex unbinding in 2-dimensions [2]. As the comprehensive review of Boucher (these proceedings) shows, the experimental support for the basic predictions of rather simple soliton models in ferromagnetic and antiferromagnetic, easy-plane chain cases is indeed very strong, even to the extent that controlled studies of impurity effects on soliton diffusion are possible. Furthermore, a similarly satisfying picture is beginning to emerge for vortex gas phenomenologies applied to quasi-two-dimensional magnets [3]. Nevertheless, theoretical analysis persistently suggests that corrections to ideal (e.g. sine-Gordon) descriptions [4] are very strong in experimentally relevant circumstances. In the absence of a complete theoretical analysis of quantum statistical mechanics for finite spin systems, it is important that we gain an understanding of dominant individual corrections to sine-Gordon approximations.

Here, we briefly review the effects of: (i) nonlinear out-of-easy-plane spin motions on classical dynamics (for continuous or discrete spin fields); and (ii) quantum spin S = 1/2 or 1 on thermodynamic properties (e.g. specific

heat, magnetic susceptibility). For definiteness, we restrict ourselves to one-dimensional Hamiltonians of the form [5]

$$H = \sum_n [J \vec{S}_n \cdot \vec{S}_{n+1} + A(S_n^z)^2 - g\mu_B B_x S_n^x] \qquad (1)$$

and [6]

$$H = \sum_n [J_x S_n^x S_{n+1}^x + J_y S_n^y S_{n+1}^y + J_z S_n^z S_{n+1}^z - g\mu_B B_x S_n^x] \quad , \qquad (2)$$

where the notation is conventional. Hamiltonians (1) and (2) are generally considered appropriate for materials such $CsNiF_3$ (S = 1 ferromagnet), TMMC ($(CD_3)_4NMnCl_3$; S = 5/2 antiferromagnet) and CHAB ($(C_6H_{11}NH_3)CuBr_3$; S = 1/2 ferromagnet). In all cases the exchange or local spin anisotropies are chosen such that there is an easy-plane and the magnetic field is applied in that plane. It has been customary to apply, as a first approximation, classical statistical mechanics with a field which is small compared with the anisotropy (e.g. $g\mu_B B \ll 2AS$). At low temperatures ($T \lesssim J$), the continuum limit is then approximately described by the sine-Gordon equation [5], which admits as elementary excitations small amplitude spin-waves, and nonlinear solitons (kinks or breathers).

In section II we describe the effects of out-of-plane spin motions (beyond the linear regime) on (1) for an antiferromagnet, i.e. J, A > 0. In particular we describe possible single kink-solitons and their collisions. Similar results for the ferromagnetic case are given in [7]. Section III summarizes recent results [8,9] for the thermodynamics of quantum S = 1/2 ferromagnets of the form (2) (with $|J_x| = |J_y| > |J_z|$). Some similar discussion of S = 1 ferromagnets is given in [9,10]. Section IV contains remarks on the outlook for nonlinear effects in spin chains.

II. Classical Dynamics in an Easy-Plane Antiferromagnetic Chain

Neutron scattering experiments [11] on TMMC have shown an interesting "cross-over" behavior of the in-plane and out-of-plane spin-wave dispersions as an in-plane magnetic field is increased. In model (1) this can be understood as a switching of the hard axis from the dipole anisotropy axis to the applied field axis [12].

This switching is also expected to affect the relative energies of the nonlinear soliton, or "kink" excitations. These kink excitations have been described in a continuum limit by an approximate mapping to the sine-Gordon (SG) equation, and are rotations of the spins through π around either the z-axis (XY kinks) or the field axis (YZ kinks) [13]. At the critical field the stationary XY and YZ kinks have equal energies, as do the in-plane and out-of-plane spin waves at the zone boundaries.

Previously XY and YZ kinks have been considered to be distinct solutions of the equations of motion, belonging to separate energy dispersion branches. Alternatively, here we review an Ansatz which includes the two as distinct limits of a single continuously connected dispersion curve [14,15]. Also we compare with results of a numerical integration of the discrete equation of motion, as well as presenting a linear stability analysis for YZ kinks.

Properties of continuum limit XY and YZ kinks have been given elsewhere [5,13]. Here we present a slightly different analysis for the YZ kinks.

In order to look for the YZ kink solution, it is best to use spherical polar coordinates where the field direction is the polar axis, in order to take the symmetry of the desired solution properly into account. So if the spins are parameterized in terms of x-polar spherical coordinates, then the equation of motion governing the YZ kinks has been shown to be [14,15]:

$$2(\Phi_{zz} - \tfrac{1}{4}\Phi_{tt}) = \alpha \sin 2\Phi; \quad \alpha \equiv 2A/J \quad . \tag{3}$$

This is a SG equation with c = 2, with the small angles θ, ϕ given in terms of the large angles Θ and Φ. See [14,15] for exact definitions of these angles. The YZ kink solution is

$$\Theta = 1/2\pi; \quad \Phi = \pm 2 \tan \exp \zeta \quad ; \tag{4a}$$

$$\zeta \equiv \gamma\sqrt{\alpha}\,(z-vt) \quad ; \quad \gamma \equiv (1-\tfrac{1}{4}v^2)^{-1/2} \quad . \tag{4b}$$

The YZ kink energy is approximately $E_{YZ} = 2\gamma\sqrt{\alpha} \times JS^2$. Note that the field determines the width and energy of XY kinks, whereas the anisotropy does so for YZ kinks. Both XY and YZ SG kink energies increase monotonically with velocity.

A linear stability analysis [14,15] of YZ SG kinks leads to the following decoupled eigenvalue equation for $\tilde{\Theta}$, where one has assumed small perturbations $\tilde{\Theta}$, $\tilde{\Phi}$, $\tilde{\theta}$ and $\tilde{\phi}$ from the SG profile, and $\beta \equiv g\mu_B B_x/JS$:

$$-\gamma^2\tilde{\Theta}_{\zeta\zeta} + (1-2\,\mathrm{sech}^2\zeta - \frac{\beta\gamma v}{2\sqrt{\alpha}}\,\mathrm{sech}\,\zeta)\tilde{\Theta} = \lambda\tilde{\Theta} \quad . \tag{5}$$

An instability is indicated by a bound state solution to this Schrödinger problem with an imaginary eigenfrequency, where the eigenfrequency ω is related to the eigenvalue by $\omega^2 = 4\alpha(\lambda-1) + \beta^2$. For v = 0, there is a sech ζ bound state, with zero eigenvalue. This corresponds to $\omega^2 = \beta^2 - 4\alpha$, however, and can have $\omega^2 < 0$ if $\beta < \beta_c \equiv 2\sqrt{\alpha}$, indicating a structural instability for fields less than the critical field.

For nonzero v, the potential for $\tilde{\Theta}$ is modified. The effect of nonzero v can be taken into account through first order perturbation theory. A short calculation shows that the stability criterion becomes $v/c > (4\alpha - \beta^2)/(\pi\beta\sqrt{\alpha})$.

The XY and YZ kinks can be connected through a variational Ansatz, made in terms of the xyz spin components in a manner similar to that done for the easy-plane ferromagnetic kinks [16]. Further motivation and details of this Ansatz calculation are given elsewhere [14,15]. Essentially, a kink profile can be represented by a trajectory of the spin vectors on the unit sphere, plus information about the distribution of the spin vectors along the trajectory. Specifically, there will be one trajectory for each sublattice, and we assume that the A sublattice spin trajectory lies in a plane at an angle θ_A to the easy plane, while the B sublattice spin trajectory lies in a plane at angle θ_B. The distribution of the spins along these trajectories is taken to be SG-like; the angular position within these tilted planes being $\phi = 4 \tan^{-1}\exp[(z-vt)/w]$, where w is a width variational parameter. Thus the Ansatz involves three parameters: θ_A, θ_B and w, and for given α and β, these are determined by locating the extrema of the Langrangian.

In Fig. 1 we show E(v) as obtained from this Ansatz using $\alpha = 0.04$ as appropriate for TMMC and for fields $\beta = 0.3$, 0.4 and 0.5 ($\beta_c = 0.4$), and for $0 < \theta_A < \pi$. We also show results from numerical integration of the equations of motion on a discrete lattice, using Ansatz profiles as initial conditions, and time averaging the kinks in their own reference frame to remove spin wave contributions to the energy (a result of having only an approximate traveling wave initial condition).

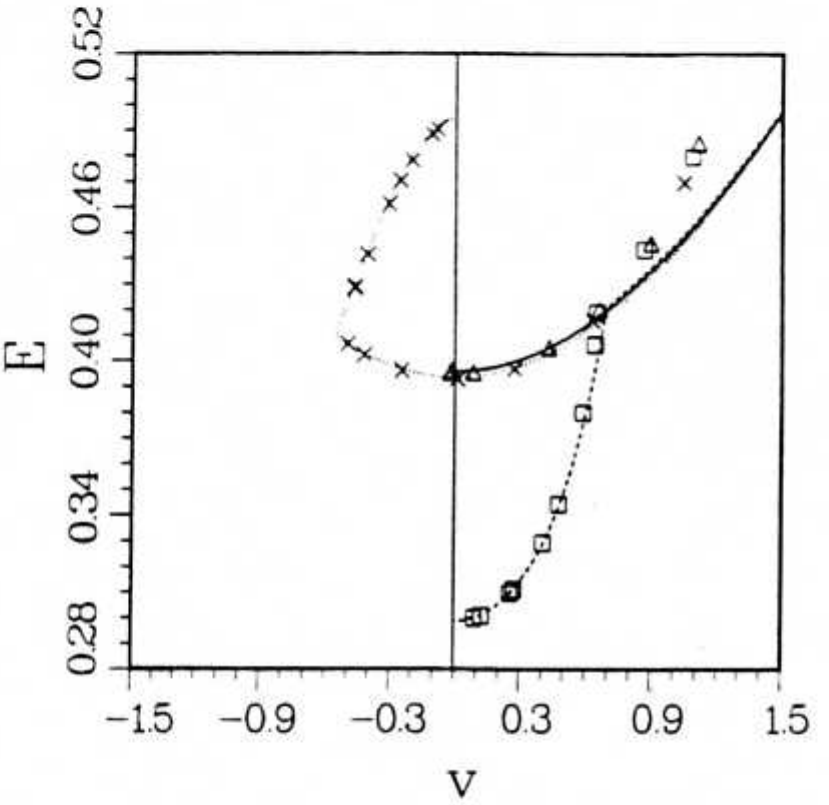

Fig.1. Some typical easy-plane antiferromagnet kink energy-velocity dispersion relationships, at three different fields. The data points were obtained from numerical integrations with $A/J = 0.02$, and $B/B_c = 0.75$ (□), 1.0 (Δ), and 1.25 (×). The curves are the corresponding results from a variational Ansatz calculation. The energy is measured in units of JS^2, and the velocity in units of $JS/\hbar$.

It is found from these numerical studies that the stable kink profile given by the Ansatz can correspond to either an XY or YZ kink, depending on θ_A; the XY and YZ branches are continuously connected. Also, for $\beta < \beta_c$, where static YZ kinks are unstable, there can be stable moving YZ kinks, consistent with the linear stability analysis results.

From the numerical integrations XY kinks are stable above and below the critical field, for $\alpha = 0.04$, $0.08 \leq \beta \leq 0.6$ and $|v/c| < 1$. Even for $\beta > \beta_c$, they show no tendency to decay to lower energy YZ kinks. Whether they can be viewed as slightly perturbed SG kinks is doubtful, especially for $\beta > \beta_c$. The situation is the same as in the ferromagnet above the critical field, where the kinks are dynamically stable but move in a direction opposite to that predicted by SG theory [7]. We conclude the XY kinks are not adequately

described by SG theory, and that there is no structural instability at the critical field.

For small velocities $v \ll c$, a two parameter Ansatz for YX kinks (putting $\theta_A + \theta_B = \pi$) reproduces the velocity dependence of the energy given by SG theory. SG theory adequately describes the YZ branch. Static YZ kinks are stable only if $\beta > \beta_c$. Dynamics YZ kinks require a minimum applied field to be stable, where this minimum field decreases with increasing velocity.

The limited extent of the XY branch could be interpreted to mean that SG-like XY kinks with larger (absolute value) velocities are dynamically unstable. Note that it is possible to estimate the stability limit for the XY kinks from the linear stability analysis for YZ kinks, since the two dispersion curves end where they intersect. First order perturbation theory for the moving YZ kink linear stability problem estimates the velocity v^*, at which the XY branch meetings the YZ branch, as

$$v^*/c_0 = \frac{2}{\pi} \frac{B_c}{B} \left[1 - \left(\frac{B}{B_c}\right)^2\right] \quad , \tag{6a}$$

where

$$c_0 = 2JS/\hbar \quad , \tag{6b}$$

and the critical field is

$$B_c = [8AJS^2]^{1/2}/(g\mu_B) \quad . \tag{7}$$

The lattice spacing is taken as the unit of length here. Note that for $B < B_c$, when $v^* > 0$, the XY effective mass is positive, while for $B > B_c$, when $v^* < 0$, the XY effective mass is negative. Equation (6a) is an approximate expression which is most accurate for B near B_c. Also note that one cannot determine v^* by equating the predicted SG XY and YZ energies for a given field; the SG theory predicts that the branches do not cross except for B very near B_c. The non sine-Gordon behavior manifests itself by strongly changing the effective masses of the XY kinks.

The XY kinks are in many ways analogous to the kinks of the easy-plane ferromagnet. The ferromagnetic kink's effective mass changes sign at a corresponding critical field, the absolute values of the effective masses are much smaller than predicted by SG theory, and they are also dynamically stable even for fields greater than the critical field. Also, while the XY kinks obey dynamics very different from SG-like, the YZ kinks, on the contrary, can be described quite accurately using SG dynamics outside of the unstable regimes mentioned. The YZ kinks have no natural analogue in the ferromagnet.

Turning to kink-antikink ($K\bar{K}$) collisions, only numerical results are presently available. We have used chains with 101 to 501 lattice sites [17], where the kink width varies as $w \sim 2JS/(g\mu_B B)$ for XY kinks and as $w \sim \sqrt{J/(2A)}$ for YZ kinks. Using a fixed ratio $2A/J = 0.04$, the field ranged from $B/B_c = 0.10$ to $B/B_c = 1.50$. For TMMC, this corresponds to 9.0 kG $\leq B \leq$ 140 kG, with $B_c \sim 90$ kG. The initial condition was an Ansatz profile for some specified parameter θ_A, where θ_A determines the tilt of the spins out of the easy plane on the A-sublattice [14,15]. The resulting profile could correspond to either an XY or YZ kink, depending on whether θ_A was near zero or $\pi/2$. At some

intermediate value of θ_A, the Ansatz kink switched from the XY branch to the YZ branch. A given combination of θ_A and B/B_c then determined the initial velocity, energy, and width of the kink.

Neumann boundary conditions were applied to the xyz spin components with the spatial derivatives on each sublattice separately set to zero at the boundaries. Classification of the type of collision was based on viewing the time evolution of the spin profile and the spatial averages of in-plane and out-of-plane angles. The tilt of the two spins at the center of one kink, one on each sublattice, measured from the easy plane, provided an additional diagnostic.

Possible outcomes of collisions include SG-like transmission, annihilation, and reflection. Some typical cases of each of these are shown in Figs. 2-4, in terms of the in-plane (ϕ) and out-of-plane (θ) angles on one sublattice. Results from these simulations are summarized in the final state phase diagram of Fig. 5.

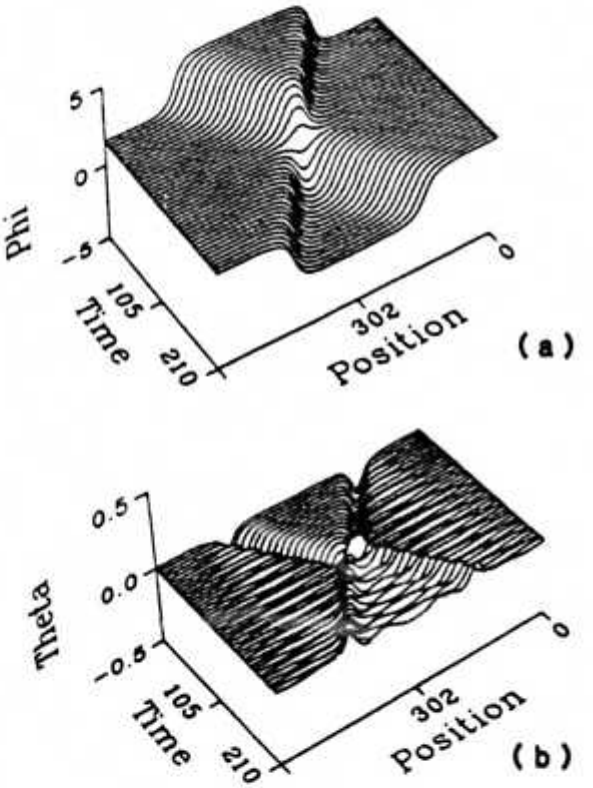

Fig. 2. $K\bar{K}$ collision of an XY-like pair, resulting in SG-like transmission; at field $B/B_c = 0.25$, with initial velocity $v_0 = 1.4$ (or $\theta_A = 0.180243$). The angle ϕ within the easy plane (on one sublattice) is shown in (a), and the associated out of easy plane angle θ is shown in (b).

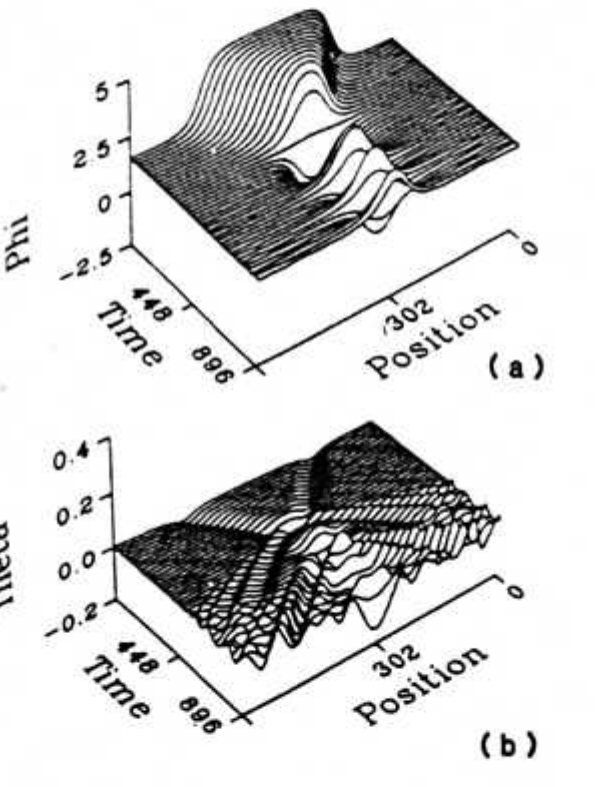

Fig. 3. $K\bar{K}$ collision of an XY-like pair resulting in annihilation; at field $B/B_c = 0.25$, with initial velocity $v_0 \leq 0.37$ (or $\theta_A = 0.024673$). Parts (a) and (b) are as described in Fig. 2. Note the oscillations, suggestive of formation of a breather-like bound state.

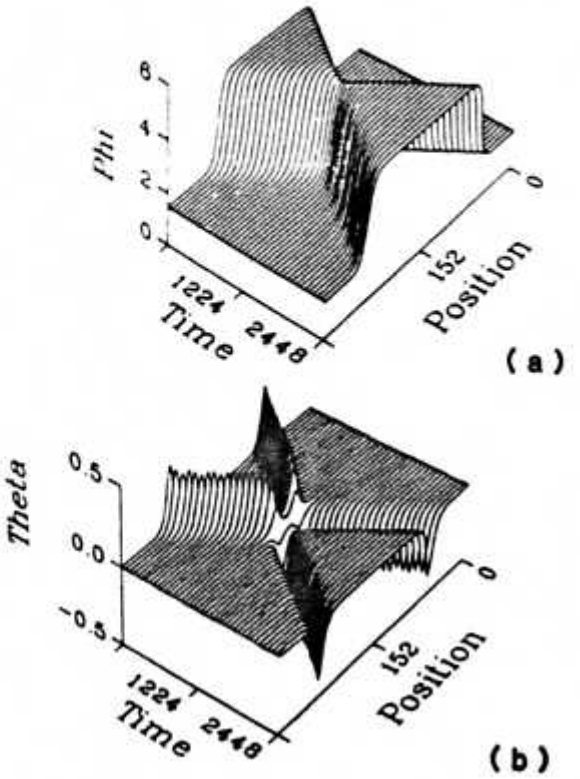

Fig. 4. $K\bar{K}$ collision of an XY-like pair also resulting in reflection, but for $B/B_c = 1.075$, with $v_0 = 0.06$ ($\theta_A = 0.364563$). Parts (a) and (b) are as described in Fig. 2.

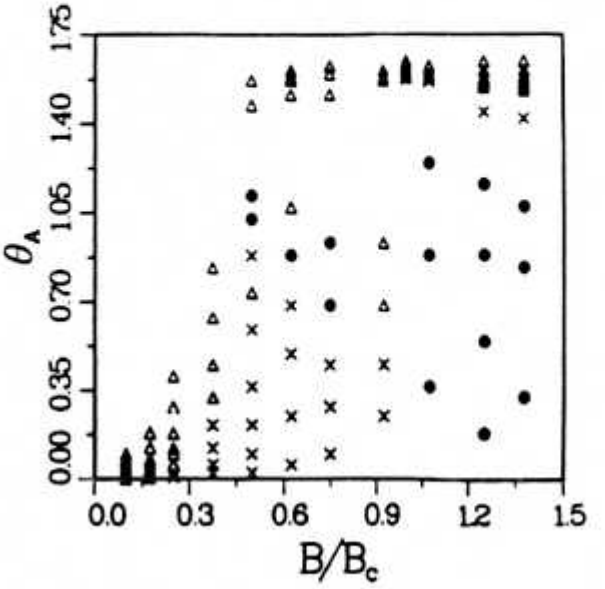

Fig. 5. An output state "phase diagram" in terms of the applied field B/B_c and the Ansatz parameter θ_A (approximately equal to the tilt of the spins out of the easy plane at the kink center). The symbols refer to transmission (Δ), annihilation (×) and reflection (o).

The results for XY kinks are similar to ferromagnetic kinks. Generally, for low fields $B < B_c$ there is SG-like transmission (Fig. 2). At higher fields, but still with $B < B_c$, the low velocity pairs annihilate, or possibly form breathers, (Fig. 3) while the higher velocity XY kinks undergo SG-like transmission. Some cases with $B < B_c$ resulted in reflection of XY kinks. For $B > B_c$, the negative effective mass XY kinks reflect, as in the ferromagnet (Fig. 4). Most of the cases tested for YZ $K\bar{K}$ pairs resulted in transmission, consistent with their nearer-SG behavior. The exceptions included some cases at small velocity for $B > B_c$, where annihilation occurs. See [17] for further details of these results.

III. Quantum Thermodynamics for Easy-Plane Ferromagnetic Chains

When using a model such as (2) to describe materials such as S = 1/2 CHAB [[6]; $J_x = J_y = -110$ K, $J_z/J_x = 0.95$], it is natural to consider that quantum effects may be important. One approach is to reintroduce quantum mechanics by replacing the classical sine-Gordon equation with its quantized version, leading to a reduction of the effective SG soliton rest mass. Alternatively, Johnson and Wright [18] reviewed the Bethe Ansatz method [19] applied to solving the quantized SG equation relevant to easy-plane ferro- and antiferromagnets -- a similar rest mass reduction is found, but still theory and experiment for CHAB, $CsNiF_3$ and TMMC disagree (for specific heat, and therefore probably for other thermodynamic properties). These

authors point out, in particular, that the corrected classical SG theory, including kink-kink interactions [20], would require a rest mass increase to bring the calculated specific heat into agreement with experiment for CHAB. This approach of quantizing a particular limit of the full classical Hamiltonian (the SG limit) seems questionable. By so doing, the out-of-plane degree of freedom is not treated properly; it is essentially transformed to a linear degree of freedom. In view of continuing concerns over the importance of out-of-plane classical motions (c.f. section II) verses the quantization of the SG model, it seems necessary to include both out-of-plane and quantum aspects simultaneously.

One way of achieving this is to use the recently developed Trotter-Suzuki transformation, whereby the thermodynamics of the original 1-D quantum system is mapped onto the thermodynamics of a 2-D classical system [21]. Numerical evaluation of the internal energy, specific heat, etc. is carried out by using either Monte Carlo or transfer matrix methods [22]. Although this will give no direct information about the excitations, (e.g., the question of existence of solitons) it can nevertheless give crucial indications of the importance of quantum effects and the validity of the assumed Hamiltonians. Attempts to implement Trotter-Suzuki formalisms for S = 1/2 and S = 1 ferromagnets are reported in [8,9,14,22]. Here we limit the discussion to an alternative "numerically exact" quantum transfer matrix (QTM) method [9,23] applied to S = 1/2 CHAB thermodynamics (model 2). We have used a technique to extrapolate from the finite size lattice to the infinite limit in both directions on the 2-D lattice, thereby making this preferred over the previous S = 1/2 quantum Monte Carlo (QMC) method [8]. We find that there is no value of exchange anisotropy from 4% to 10% for which the QTM results for specific the peaks will agree with experiment. We have, however, tested that the QTM calculation gives results consistent with the QMC calculation. The computing method used was given by Betsuyaku [23], who adapted that of Morgenstern and Binder [24] as originally applied to spin glass models, by allowing for the four-spin interactions. It is necessary to choose free boundary conditions in the spatial direction (N), while periodic boundary conditions are imposed in the Trotter direction (m) as a result of the trace. The method requires storing 2^{2m} Boltzmann factors -- for this calculation we have used $1 \leq m \leq 9$. (The integer m is the lattice size in the Trotter direction.) Computing time rises exponentially with m and linearly with N. Presently the practical limit is m = 9 for storage as well as CPU time using a CRAY-1 800 K word machine, while $N > 100$ is no practical problem. Extrapolations for $N, m \to \infty$ are discussed in [9,23].

First the method was tested for $m_1 = 8$, N = 32, at 5% anisotropy ($J_z/J_x = 0.95$) to compare with previous spin-$\frac{1}{2}$ QMC data [8,14]. Results for internal energy, specific heat, magnetization and susceptibility all agreed to within about 5% over the temperature range 4 K to 20 K. Then we applied this method to model (2) with anisotropy ranging from 4% to 10%, in order to compare with the experimental specific heat data of Kopinga et al. [6]. The difference specific heat $C(B) - C(0) = \Delta C$, is plotted versus field for a series of temperatures, and then the peak position and height are determined and plotted verses T^2 and T respectively. Some representative ΔC verses B curves are shown in Figure 6, for the case of 5% anisotropy. The data lie on smooth curves, making the determination of peak positions and heights possible. Interpolation, using a parabolic fit to the peaks, provided a simple accurate way to determine the heights and positions. In Figure 7 the resulting B_{peak} and ΔC_{max} are shown, for anisotropies 4%, 5%, 6%, 8%, and 10%, and compared with classical SG theory and experiment.

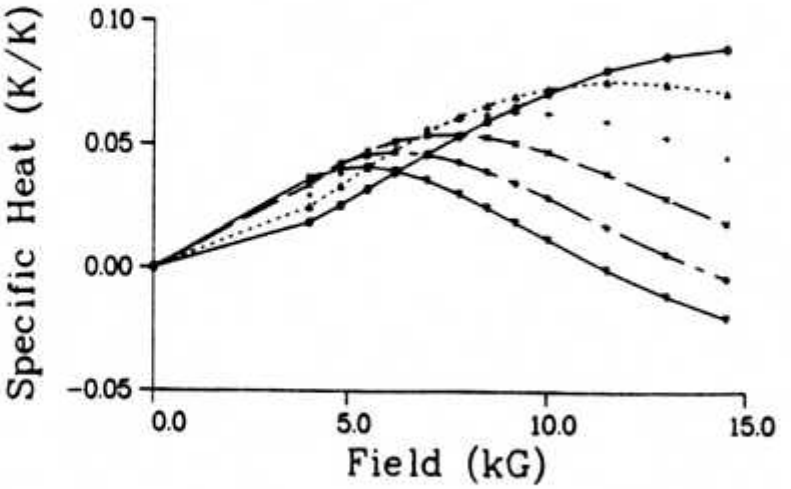

Fig. 6. Some typical results for ΔC vs. B as obtained with the spin-1/2 QTM calculation using CHAB parameters (5% anisotropy). The data correspond to temperatures T = 4.0 K (∇), 4.4 K ($\Diamond$), 4.9 K (x), 5.5 K (+), 6.2 K (Δ) and 7.2 K (0), and have been extrapolated to $N \to \infty$, $m \to \infty$.

The dashed lines in Figure 7 are classical SG theory results using a soliton rest mass $E^{\circ}_{SG} = 8(JS^3 g\mu_B B)^{1/2}$, that is, with no adjusted parameters, as in [20]. The predictions of classical SG theory are independent of the anisotropy. Expressions given by Sasaki and Tsuzuki [20] include contributions from spin waves, solitons, and soliton-soliton interactions. Their calculations predict that the general result for a SG ferromagnetic is

$$B_{peak} = AT^2 \quad , \quad A = (64 t_m^2 g\mu_B JS^3)^{-1} \quad , \tag{8}$$

where $t_m = T/E^{\circ}_{SG} = 0.190$ has determined the peak position. The corresponding peak height is found to be given by

$$\Delta C_{max} = A'T \quad , \quad A' = 0.196/JS^2 \quad . \tag{9}$$

We see that agreement between this classical theory and experiment is fair for B_{peak} but not as good for ΔC_{max}. None of the chosen values of anisotropy for the QTM fit well to the experimental CHAB data over this temperature range. If the SG soliton rest mass is ad-hoc renormalized such that the slopes of the SG theory B_{peak} curves agree with the experimental slope, then the implied changes in the SG theory ΔC_{max} are not adequate to cause them to simultaneously fit the experimental data. It has not been apparent how to resolve this problem with classical SG theory. The QTM data presented here obviously should require no such quantum renormalization, but nevertheless systematically disagree with experiment, casting some doubt on the adequancy of the customary model (2). Quantum Monte Carlo studies for S = 1 $CsNiF_3$ [9,14] raise similar questions. (QTM methods of the form used for S = 1/2 are presently impractical for S = 1 because of computer memory limitations.)

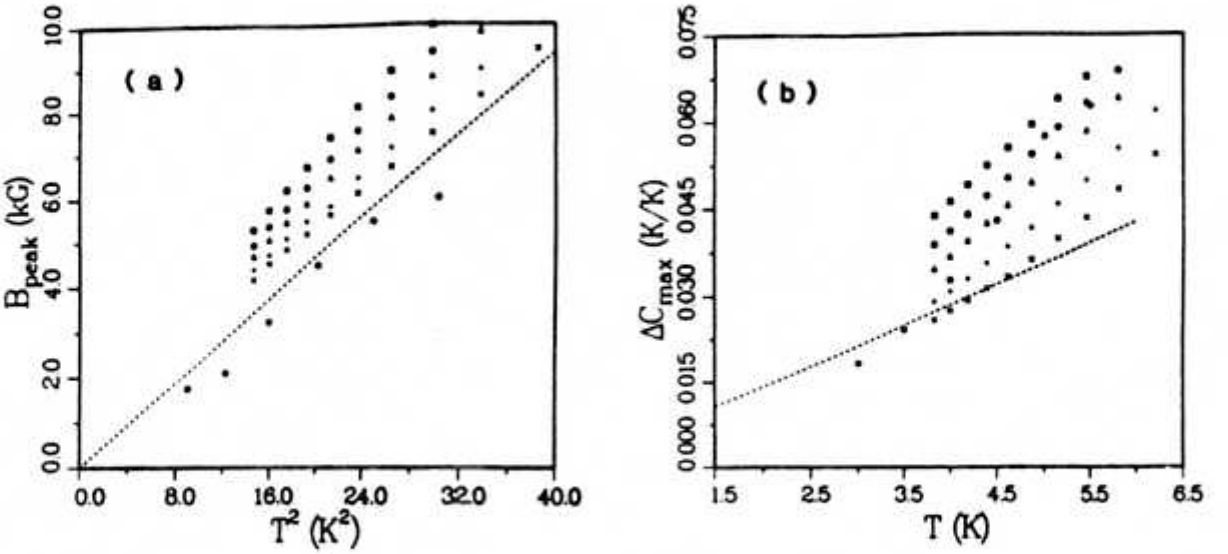

Fig. 7. Spin-1/2 QTM results for (a) B_{peak} and (b) ΔC_{max}, using model (2) with $J_x = J_y = -110$ K, for a series of values of anisotropy $J_z/J_x = 0.96$ (□), 0.95 (◇), 0.94 (△), 0.92 (+) and 0.90 (x). These are all data from the extrapolation to $N \to \infty$, $m \to \infty$. The solid data points (●) are the experimental data on CHAB by Tinus et al. [25]. The dashed lines are the classical SG theory of Sasaki and Tsuzuki [20].

IV. Outlook

In view of the results summarized in sections II and III, we should be surprised how well classical sine-Gordon theory can explain experimental data on materials such as CHAB, TMMC and $CsNiF_3$ with easy-plane applied magnetic fields. For instance, we have seen that the quantized version of the ferromagnet Hamiltonian gives approximately the same low-T thermodynamics as the classical SG Hamiltonian, for the case of S = 1/2 CHAB. This can be compared with classical transfer matrix calculations [25] for the ferromagnet Hamiltonians, which give <u>much</u> larger low-temperature specific heat peaks. We tentatively conclude that the quantum mechanics plays a strong role in restricting the spins to the easy plane (including a zero-point out-of-plane component) thereby making the classical theory more appropriate than might at first be expected. It will be interesting to see whether such a restriction also controls <u>dynamics</u> quantum properties, e.g. as measured in inelastic neutron scattering. In the context of quantum Monte Carlo simulations, this will require solving the outstanding problem of Laplace inversion from a finite imaginary time interval.

We anticipate that low-dimensional magnetic materials will continue to develop as accessible contexts in which to investigate fundamental nonlinear and nonequilibrium processes, including: (i) effects of impurities and damping mechanisms on soliton transport (c.f. Boucher); space-time coherence and chaos (e.g. breather selection and synchronization by an external oscillatory field [26], or competing spin interactions leading to inhomogeneous structures and associated dynamics, or chaotic dynamics [26], or even "quantum chaos" [27]); and (iii) vortex-spin-wave <u>dynamics</u> in quasi-<u>two</u>-dimensional magnets [3], which is especially timely in view of the emergence of many

well-characterized materials and improved resolution inelastic neutron scattering data.

References

1. M. Steiner, K. Kakuri and J. K. Kjems, Z. Phys. B 53, 117 (1983); J. P. Boucher, L. P. Regnault, J. Rossat-Mignod, J. P. Renard, J. Bouillot, W. G. Stirling, and F. Mezei, Physica 120B, 241 (1983).
2. J. M. Kosterlitz and D. J. Thouless, J. Phys. C 6, 1181 (1973); and Prog. Low Temp. Phys. (D. F. Brewer, ed.), Vol. VIII B, North-Holland, Amsterdam (1978).
3. C. Kawabata, M. Takenchi and A. R. Bishop, J. Magn. Magn. Mat. 54-57, 871 (1986); A. R. Bishop et al., in preparation.
4. See, for example, P. Kumar, Phys. Rev. B 25, 483 (1982); Physica 5D, 359 (1982); E. Magyari and H. Thomas, Phys. Rev. B 25, 531 (1982); J. Phys. C 16, L535 (1983).
5. H. J. Mikeska, J. Phys. C 11, L29 (1978); 13, 2913 (1980).
6. K. Kopinga, A. M. C. Tinus and W. J. M. de Jonge, Phys. Rev. B 29, 2868 (1984).
7. G. M. Wysin, A. R. Bishop and P. Kumar, J. Phys. C 17 , 5975 (1984); 15, L337 (1982).
8. I. Satija, G. M. Wysin and A. R. Bishop, Phys. Rev. B 31, 3205 (1985).
9. G. M. Wysin and A. R. Bishop, Phys. Rev. B 34, 3377 (1986).
10. G. Kamienarz and C. Vanderzande, preprint (1986).
11. I. U. Heilmann, R. J. Birgeneau, Y. Endoh, G. Reiter, G. Shirane and S. L. Holt, Solid State Commun. 31, 607 (1979).
12. I. Harada, K. Sasaki and H. Shiba, Solid State Commun. 40, 29 (1981).
13. N. Flüggen and H. J. Mikeska, Solid State Commun. 48, 293 (1983).
14. G. M. Wysin, PhD. Thesis, Cornell University (1985).
15. G. M. Wysin, A. R. Bishop and J. Oitmaa, J. Phys. C 19, 221 (1986); J. Magn. Magn. Mat. 54-57, 831 (1986).
16. R. Liebmann, M. Schöbinger and D. Hackenbracht, J. Phys. C 16, L633 (1983).
17. G. M. Wysin and A. R. Bishop, in preparation.
18. M. D. Johnson and N. F. Wright, Phys. Rev. B 32, 5798 (1985).
19. M. Fowler and X. Zotos, Phys. Rev. B 25, 2805 (1982).
20. K. Sasaki and T. Tsuzuki, J. Magn. Magn. Mat. 31-34, 1283 (1983).
21. M. Suzuki, Prog. Th. 1454 (1976); M. Barma and B. S. Shastry, Phys. Rev. B 18, 3351 (1978).
22. For examples, see J. J. Cullen and D. P. Landau, Phys. Rev. B 27, 297 (1983); H. DeRaedt, A. Lagendijk and J. Fivez, Phys. Rev. B 46, 261 (1982).
23. H. Betsuyaku, Prog. Th. Phys. 73, 319 (1985); Phys. Rev. Lett. 53, 629 (1984).
24. I. Morgenstern and K. Binder, Phys. Rev. B 22, 288 (1980).
25. M. G. Pini and A. Rettori, Phys. Rev. B 29, 5246 (1984); A. M. C. Tinus, W. J. M. de Jonge and K. Kopinga, preprint (1985); Phys. Rev. B 32, 3154 (1985).
26. A. R. Bishop and P. S. Lomdahl, Physica D 18, 54 (1986); G. M. Wysin and A. R. Bishop, J. Magn. Magn. Mat. 54-57, 1132 (1986).
27. K. Nakamura et al., Phys. Rev. B 33, 1963 (1986); Phys. Rev. Lett. 57, 5 (1986).